

Optical Detection Systems on Microfluidic Chips

Hongwei Gai, Yongjun Li, and Edward S. Yeung

Abstract Optical detection continues to dominate detection methods in microfluidics due to its noninvasive nature, easy coupling, rapid response, and high sensitivity. In this review, we summarize two aspects of recent developments in optical detection methods on microfluidic chips. The first aspect is free-space (off-chip) detection on the microchip, in which the conventional absorption, fluorescence, chemiluminescence, surface plasmon resonance, and surface enhanced Raman spectroscopies are involved. The second aspect is the optofluidic (inside-chip) detection. Various miniaturized optical components integrated on the microfluidic chip, such as waveguide, microlens, laser, and detectors are outlined.

Keywords Lab-on-a-chip · Optofluidic · Point of care

H. Gai (✉)

School of Chemistry and Chemical Engineering, Xuzhou Normal University, Xuzhou 221116, China

and

State Key Laboratory of Chemo/Biosensing and Chemometrics, Hunan University, Changsha 410082, China

and

School of Biology, Hunan University, Changsha 410082, China

e-mail: gaihw@hnu.cn

Y. Li (✉)

State Key Laboratory of Chemo/Biosensing and Chemometrics, Hunan University, Changsha 410082, China

and

School of Chemistry and Chemical Engineering, Hunan University, Changsha 410082, China

e-mail: liyongjunef@gmail.com

E.S. Yeung

State Key Laboratory of Chemo/Biosensing and Chemometrics, Hunan University, Changsha 410082, China

and

School of Biology, Hunan University, Changsha 410082, China

Contents

1	Introduction	173
2	Conventional Free-Space Optical Detection	173
2.1	Absorbance Detection	173
2.2	Fluorescence Detection	176
2.3	Chemiluminescence	181
2.4	Surface Plasmon Resonance and Localized Surface Plasmon Resonance	182
2.5	Surface Enhanced Raman Spectroscopy/Imaging	184
3	Detection Inside the Chip	185
3.1	Planar Optical Waveguide	186
3.2	Micro lens	189
3.3	Optofluidic Laser	193
3.4	Optical Detector	195
4	Conclusions	197
	References	197

Abbreviations

μ -TAS	Micro total analysis system
ARROWs	Antiresonant reflecting optical waveguides
CCD	Charge-coupled device
CE	Capillary electrophoresis
CL	Chemiluminescence
CMOS	Complementary metal-oxide-semiconductor
DFB	Distributed feedback
HRP	Horseradish peroxidase
L ² waveguide	Liquid-core/liquid-cladding waveguide
LCW	Liquid-core waveguide
LED	Light-emitting diode
L-GRIN	Liquid gradient refractive index
LIF	Laser-induced fluorescence
(L)SPR	(Localized) surface plasmon resonance
OFM	Optofluidic microscopy
OPD	Organic photodiode
PC	Photonic crystal
PDMS	Poly(dimethylsiloxane)
PMMA	Poly(methyl methacrylate)
PMTs	Photomultiplier tubes
QD	Quantum dot
SERS	Surface enhanced Raman spectroscopy
UV/Vis	Ultraviolet-visible

1 Introduction

Microfluidic chips have the potential to integrate all experimental processes in a research laboratory (sample preparation, reaction, separation, and detection) onto a microscale device. Ever since the micro total analysis system (μ -TAS) was firstly proposed by Manz et al. in the early 1990s [1], it has achieved great advances in many scientific research fields, such as medical diagnostics [2], drug screening [3], proteomics [4], and environmental and food analysis [5, 6]. To be able to read out the analytical results captured by a microchip, the detection system is the core part and is responsible for signal acquisition. To date, various detection modules including optical detection, electrochemical detection, mass spectrometry and others, have been assembled or partly assembled onto the microchip. The ultimate goal of having the detection system on the microfluidic chip is to incorporate it as an inseparable part of a portable microdevice with high sensitivity and fast response.

In this review, we mainly focus on the recent developments in optical systems assembled onto a chip because optical detection is easily implemented in chemical/biochemical laboratories, has acceptable sensitivity in regular analysis, and simplicity in coupling with other functional units. Such topics have been touched on in previous reviews. A general overview of earlier detection methods has been published elsewhere [7, 8]. The specialized subjects of optical systems such as detectors for separation and unconventional detection can be found in the literature [9–11]. The current optical detection systems on microfluidic chips can be summarized from two perspectives. The first is the traditional optics configuration strategy also called “off-chip” or “free space,” in which light propagates in air before and after interaction with the sample (see Sect. 2). In this mode, the detection units (e.g., light source, mirrors, and detectors) are separated from the chip platform. We present the detection methods of absorption, luminescence and scattering in Sects. 2.1–2.5. The second strategy is the “on-chip” mode, in which the optics are integrated with or fabricated together with the fluidic functional units (see Sect. 3). When the optical property of the integrated optics can be tuned by fluidic technology, the microfluidic is also called “optofluidic.” This mode, however, is in the development stage, and a highly integrated optofluidic is not fully realized yet. Some related optical components such as waveguides, microlens, detectors and microscopes will be discussed in Sects. 3.1–3.4. The nonoptical detection methods (e.g., electrochemical detection, mass spectrometers, and nuclear magnetic resonance) are not covered in this review but can be found in previous reviews [7, 8, 12].

2 Conventional Free-Space Optical Detection

2.1 Absorbance Detection

UV/Vis absorption spectroscopy is the most straightforward and popular detection method in separation and microseparation science due to its generality, sensitivity,

and adequate detection limit. Absorption spectra are related to the structure and concentration of the analyte and are based on the capability of samples to attenuate the incident electromagnetic radiation at various wavelengths.

The depth of the channels in microchips is relatively shallow compared to their width due to the character of the fabrication method. If light is designed to pass through the channel perpendicular to the chip plane, the optical length through the sample is limited by the depth of the channel, which is shortened from millimeters in conventional analysis to tens of micrometers in microanalysis, adversely impacting the sensitivity. To address the issue of the low sensitivity caused by a short optical length, various approaches were developed to increase the optical path length.

With free-space optics, light first propagates in the air and then enters the detection cell. The optical length is enlarged simply by changing the geometry of the channel at the detection point, such as incorporating a short, wide bubble cell within the channel [13], or sandwiching an additional glass substrate with a through-hole at the detection point to increase the optical length in the vertical direction of the chip plane [14]. Despite that, these methods suffer from the limited improvement of optical length because the changes of channel geometry are detrimental to maintaining separation efficiency and to blocking stray light. Introducing the light along the channel axially is a practical alternative for enhancing absorbance. The light can be reflected between two mirrors by coating 200- μm aluminum films above and below the channel. Effective optical lengths ranging from 50 to 272 μm were achieved by adjusting the angle of laser incidence (Fig. 1) [15]. Billot et al. implemented a similar idea on a glass–PDMS–glass microchip by coating the mirrors on the inside surfaces of the channel and exciting the sample with a normal illumination configuration [16]. Besides making light reflect multiple times inside the channel, passing light along the channel axially in a straight line is another way of increasing the optical length. This idea is implemented by fabricating two parallel 45° mirrors at each end of the microchannel so that light was

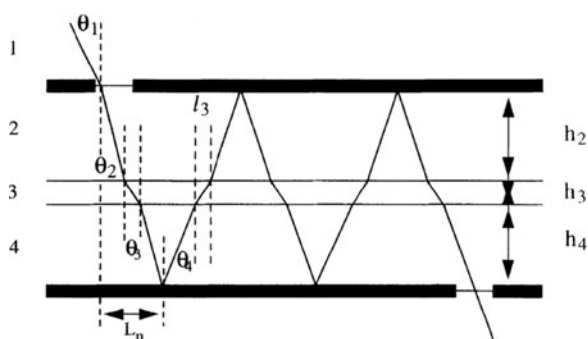


Fig. 1 Diagram showing a planar multireflection absorbance cell. Aluminum mirrors (*thick lines*) were coated above and below a channel. The narrowest region inside the cell is the fluid flow path (Reprinted from [15] with permission of Wiley-VCH). i (1,2,3,4) refers to different medium; θ_i is the angle within the medium i with respect to the surface normal; h_i is the thickness of the medium i ; l_i is the longitudinal distance in each of medium and $l_i = h_i \tan(\theta_i)$; L_n is the total longitudinal travel for once reflection; n the total number of reflections

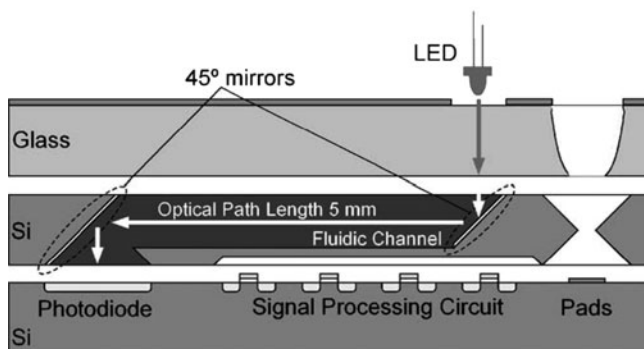


Fig. 2 Cross-sectional diagram of a microchip. Two parallel 45° mirrors were fabricated at each end of the microchannel to increase the optical length (Reprinted from [17] with permission of Elsevier)

reflected into the channel and out to the detector by the mirrors, making the 5-mm channel the optical path (Fig. 2) [17]. Within this category, other efforts were also made to improve the sensitivity of UV absorption and to maintain the high separation performance of microscale electrophoresis. For examples, Lin et al. fabricated a hybrid poly(dimethylsiloxane) (PDMS)/quartz chip with a 100- μm thick PDMS membrane on the detection window for UV absorbance detection [18]; Ou et al. developed a PDMS/SU-8/quartz hybrid chip incorporating UV absorbance-based whole-channel imaging detection [19].

Embedding waveguide optics into the microchannel is another way to enlarge the optical length. Integrated waveguides on-chip are similar to electrical circuits on electronic chips, carrying information about the analytes. This has good potential for design of a lab-on-a-chip because it can realize the practical miniaturization of the optical elements. Actually, one of the initial motivations for developing waveguides was to extend the optical length by coupling the light effectively into the axial direction of the channel. The channel length then becomes the light path length. Integrated optical waveguides on microchips offer the capability to deliver and capture light at nearly arbitrary positions and angles on the chip. With the help of an in-plane waveguide, various absorbance detection geometries have been developed, such as a 750- μm U-cell [20], a 1,000- μm U-cell on an electrochromatography chip [21] and a hollow Abbe prism on a PDMS chip [22]. However, the enhancement of optical losses with increasing optical path length was observed because of stray light and light dispersion, leading to a reduction in the signal-to-noise ratio [23, 24]. Accordingly, a light collimating system was integrated in the front of the extended optical path to block stray light and increase the sensitivity [25]. Llobera et al. integrated optical fibers, air mirrors, and collimation microlenses on a chip to realize a multireflection absorbance detection system in which the detection limit of 41 nM for fluorescein was achieved [26]. Fang et al. provided an example of miniaturized absorbance detection. They employed a U-shape bent capillary to couple light into the capillary and out to the photodetector with less light loss and less dead volume,

resulting in a 15 mm effective optical path length, which significantly simplified the system for use as a hand-held photometer [27].

A technique based on absorbance of evanescent waves has been developed very recently, in which the evanescent field was coupled into a microchannel by a U-bend SU-8 waveguide. When the analytes flow through the evanescent field, they interact with the light and induce evanescent wave absorption. This technique is expected to also suppress the scattered light when light passes directly through the detection region, thereby enhancing the sensitivity [28].

Waveguide-based cavity ring-down absorption spectroscopy [29] can increase the optical path length by reflecting a pulse of light multiple times through the sample without changing the channel geometry, and is also a promising way for absorption detection on the microchip. In the case of the tartrazine detection, microfluidic-based fiber-loop ring-down absorption spectroscopy has shown a satisfactory detection limit of 5 μM [30, 31].

Despite the fact that absorbance is more limited in sensitivity than fluorescence, the potential of an inexpensive miniaturized optical setup still provides an advantage in certain applications, such as when changes in optical density or color are sufficient for clinical diagnosis.

2.2 *Fluorescence Detection*

Today's lab-on-a-chip devices take advantage of various optical detection strategies to achieve microvolume detection. Of these, fluorescence detection is still a preferred choice to be incorporated onto microdevices primarily due to its high sensitivity and high selectivity for cellular and molecular sensing. Fluorescence is the emission of light of fluorophores where the cycle of excitation and emission will continue until the excitation source is turned off or the fluorophore is photodecomposed. The fluorescence of biomacromolecules originates either from the native chromophore inside the molecules or from chemically linked fluorescent labels. Recently, the fluorescent labels for microanalysis have been extended from synthetic dyes, fluorescent proteins, and quantum dots (QDs) to nanoparticles. Development and exploitation of new types of fluorescent probes with high quantum yield and high specificity on lab-on-a-chip will be helpful to improve the detection sensitivity and minimize the size of optical components in the sensing system.

The complete optical setup of induced fluorescence involves an excitation part and an emission part. The intersection point of the two parts is the detection window in the microdevice. The excitation part starts from the light source and ends at the microdevice, while the emission part originates from the microdevice and stops at the detector. In free-space fluorescence detection, the common excitation sources include the laser, light-emitting diode (LED), and mercury or xenon arc lamp, and each light source has its distinctive spectroscopic property and practical benefits. Laser-induced fluorescence (LIF) is a highly sensitive optical detection method and is able to perform even single molecule detection. LIF has been introduced into the

microchip at the early stage of lab-on-a-chip and remains to be a popular approach, especially for analyzing low-abundance molecules after combining with point detectors like photomultiplier tubes (PMTs). The high pressure vapor discharge lamp is the standard light source for modern fluorescence microscopy due to its broad spectrum, ranging from UV to visible regions, and because it is less expensive and more flexible by offering different wavelengths with the assistance of proper optical filter sets. The lamp-based fluorescence microscope is usually coupled with an imaging detector like a charge-coupled device (CCD) to analyze cellular fluorescence. An LED is a small semiconductor light source and can efficiently produce light. These merits indicate that LED is suitable for integration into microfluidic chips. Yao et al. succeeded in integrating a green organic LED and thin film interference filter into a microfluidic device through layer-by-layer stacking [32], and also designed a similar LED-induced fluorescence-based microdevice for the imaging of whole-column isoelectric focusing [33] and for high throughput capillary array electrophoresis on the chip [34].

Fluorophores emit photons with 4π steradians once they are excited. Therefore, fluorescence can be collected at any solid angle by an objective or a lens. One prevalent optical configuration for induced fluorescence detection is that the collection objective in the emission part is the same as the focus components in the excitation part. Fluorescence collected by the same objective passes through the dichroic and emission bandpass filter and reaches the detector. Such configuration is called epi-illumination in fluorescence microscopy and is also the basis of confocal LIF as long as a pinhole is placed in the conjugate plane to the sample plane to block the out-of-focus light and a laser diffraction-limited spot is used to excite samples. A typical confocal LIF mode on-chip is depicted in Fig. 3 and is almost the same as for the confocal microscope except that the microchip is used to replace the microscope stage. Additionally, the emission part of another setup for fluorescence detection does not share the same objective with the excitation part, and each part has its own focusing systems. In this configuration, the collection angle seriously affects the sensitivity and has been optimized to 45° [35] by Fang's group. Subsequently, Whiting et al. determined under- and oversampling of individual particle distributions in microfluidic electrophoresis with orthogonal LIF [36]. Using this orthogonal LIF detector, a detection limit of 1,761 molecules of fluorophore was obtained under a constant flow of fluorescein. Compared to the common LIF detection scheme used with microfluidic devices, this is a significant improvement.

From the viewpoint of instrumentation development, the aim of optical detection systems of lab-on-a-chip is miniaturization, but under the premise that the detection sensitivity is maintained at a practical level. Therefore, we shall review the fluorescence detection on-chip from the points of view of improving sensitivity and miniaturization.

LIF is appropriate to deal with the minute amounts of sample in the microchannel and to demonstrate the feasibility of the concept of μ -TAS in the early stage of development [37, 38]. Optimization of detection parameters to improve the sensitivity of confocal LIF on-chip was accomplished [39] and the authors detected 300 fM fluorescein with a signal-to-noise ratio of 6.1 in continuous-flow mode and

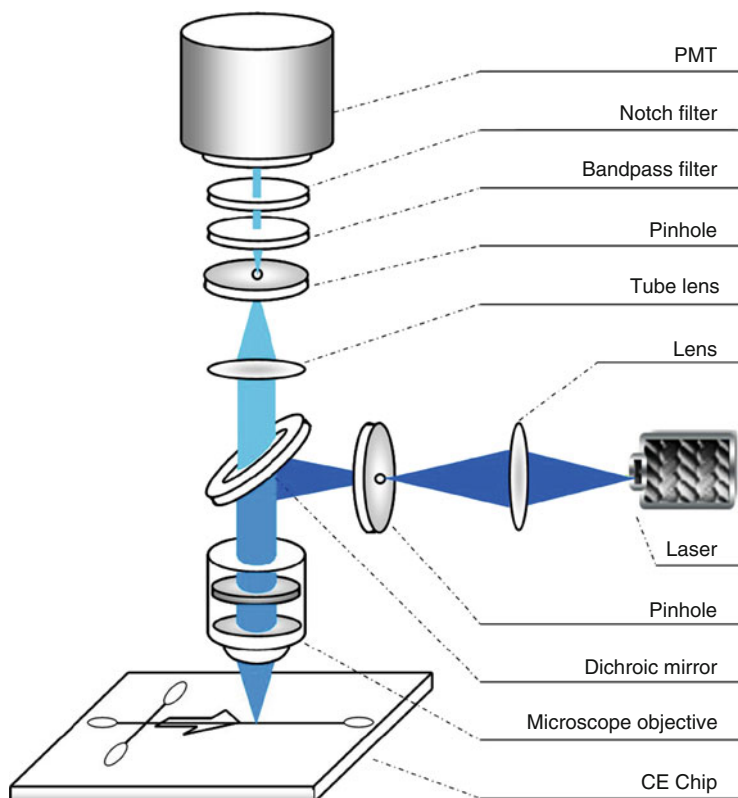


Fig. 3 Confocal fluorescence detection on a microchip. A laser was used as the excitation source. The laser light passed through a biconvex lens, was focused into an illumination pinhole, and was subsequently reflected by a dichroic mirror and focused in the channel on the capillary electrophoresis (CE) chip by a microscope objective. The fluorescence signal from the sample, collected by the microscope objective, was passed through the dichroic mirror, focused by the tube lens into a confocal pinhole, and then detected by a photomultiplier tube (PMT). To improve the signal-to-noise ratio, band-pass filter and notch filter were inserted above PMT for spectral filtering

1 pM fluorescein in capillary zone electrophoresis. Consequently, the confocal LIF was successfully used to detect single molecules of a 100–1,000 bp DNA ladder in a microchannel by electrodynamic focusing [40]. High-quality DNA sequencing separations have also been performed in microfabricated electrophoresis channels [41]. Early results of detection of single molecules labeled with organic dyes in microchannels were reviewed by Manz in 2005 [42]. The point detection mode suffers from low detection efficiency because the diffraction-limited focused laser spot is so small that the whole channel cannot be covered and most molecules do not pass through the laser beam. Chiu et al. designed a line-confocal detection geometry comprising an elliptically shaped probe volume to enlarge the fraction of molecules that flow through the laser beam without severely decreasing the

signal-to-noise ratio [43]. Another way to improve the single molecule detection efficiency in microchannels is to employ an imaging detector, either an intensified charged coupled device (ICCD) or an electron multiplied CCD (EMCCD), by imaging a larger detection area than covered by the point detector. Single moving lambda DNA molecules forced by pressure or electrokinetic flow in the microchannel are easily observed with an imaging detector [44]. When the total internal reflection excitation mode is coupled to the microchannel, the velocity of molecules near the channel wall can also be measured. Therefore, the velocity distribution in the microchannel can be profiled by adjusting the excitation depth of the evanescent wave [45–47]. In addition to organic dyes that are used as the fluorescent label, recently developed fluorescence nanoparticles are also used to label molecules. Our group has improved the fluorescence characteristic of core–shell QDs by adding thiol-group chemicals and labeled QDs to the oligonucleic acids and demonstrated the advantages of QDs for microchips [48–50].

The microdevice is also an ideal platform for single-cell analysis when the functional units of cell sampling, cell sorting, cell breakage, chemical separation, and detection are integrated onto a single chip. Meanwhile, single-cell chemical analysis on the microchip is a typical application of LIF detection on-chip. Yu developed a high-throughput single-cell analysis method on PDMS microfluidic chips to simultaneously analyze glutathione and rhodamine 123 in single K562 cells. They could analyze about ten cells each minute in one channel [51]. For nucleic acid molecules, the labeling process can be implemented in the channel by intercalating dyes into the base pairs. Kleparnik [52] assessed the effects of doxorubicin, a cytostatic, on the apoptosis of single cardiomyocyte cells by separating DNA fragments labeled with ethidium bromide. For protein molecules, label-free LIF detection is a suitable method due to the UV fluorescence of the three amino acids tryptophan, tyrosine, and phenylalanine. Hellmich reported LIF detection of native protein lysed from single cells and excited with a 266-nm laser [53]. The authors further demonstrated the CE separation of two proteins from a single cell and improved the separation efficiency and detection sensitivity by shortening the electrical lysis time and improving the injection plug size [54].

LIF detection is the most sensitive optical method so far, but is hard to miniaturize in order to satisfy the ultimate goal of a microfluidic chip that assembles all analytical processes within one micrometerscale microstructure. Therefore, how to achieve the miniaturization of fluorescence detection on microdevices is becoming an active field for lab-on-a-chip research. Several examples demonstrate recent advances in miniaturized LIF detection on the microchip. In 2005, Renzi et al. designed a hand-held microchip-based analytical instrument that combines fluidic, optics, electrical power, and interface modules and integrates the functions of fluidics, microseparation, lasers, power supplies etc., into an $11.5 \times 11.5 \times 19.0$ cm system (Fig. 4a) [55]. This device allows picomolar (10^{-11} M) detection sensitivity for fluorescent dyes and nanomolar sensitivity (10^{-9} M) for fluorescamine-labeled proteins. Novak et al. built a low-cost mini-fluorescence detection system of $30 \times 30 \times 11$ mm (Fig. 4b), in which LED, photodiode, mirrors, lenses, and electronic circuit are housed together, with

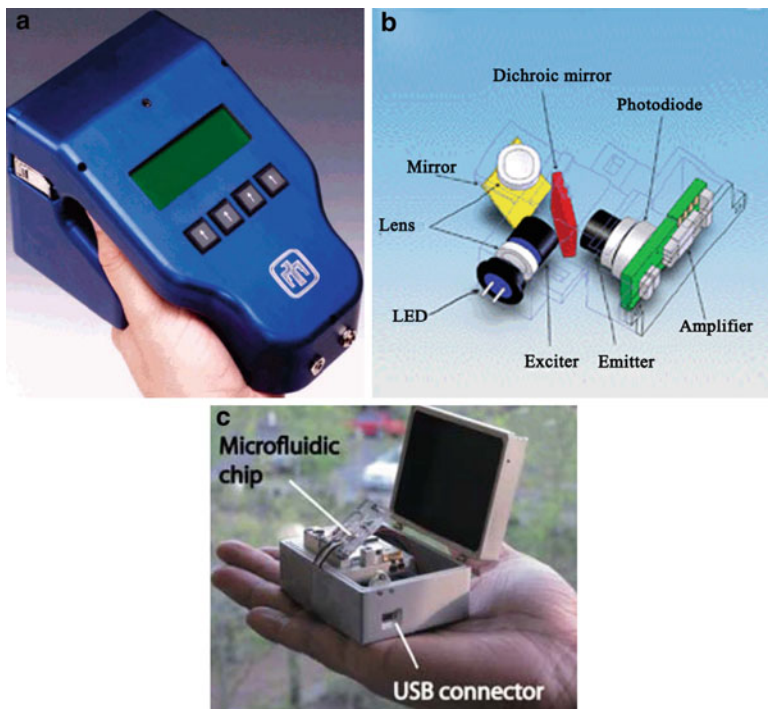


Fig. 4 Examples of portable microfluidic instruments. (a) The system integrates fluidics, micro-separation chips, lasers, optics, high-voltage power supplies, electronic controls, data algorithms, and a user interface into a hand-portable instrument (Reprinted from [55] with permission of The American Chemistry Society). (b) A miniature LED-induced fluorescence microdevice (Reprinted from [56] with permission of The Royal Society of Chemistry). (c) Hand-held isotachopheresis instrument (dimensions: $7.6 \times 5.7 \times 3.8$ cm) (Reprinted from [57] with permission of The Royal Society of Chemistry)

a sensitivity in the low nanomolar range [56]. In 2010, Backhouse et al. presented a hand-held isotachopheresis microchip device [240 g, (Fig. 4c)] with LIF detection, which was powered by a universal serial bus link connected to a laptop computer. A limit of detection of 100 pM for Alexa Fluor 647 was demonstrated [57].

Making the size of each optical component for LIF as small as possible and assembling them onto microfluidic systems is a straightforward way to develop a portable analyzer as described above. Another idea to minimize the instruments is to design and fabricate all optics directly on-chip, which means that the optics such as light source [58–60], lens [61, 62], and detector [63] are part of the microchip rather than minimizing them and interfacing them with microchip. This self-contained optical microfluidic, also called optofluidic, is reviewed in the Sect. 3 of this article.

2.3 Chemiluminescence

Chemiluminescence (CL) is a molecular luminescence spectrometry, originating from the release of energy in a chemical reaction: a metastable reaction intermediate or product in a singlet excited state relaxes to the ground state with the emission of a photon. By measuring the as-generated luminous intensity, one can conveniently determine the analyte concentration. Compared to other spectroscopic techniques, there is an absence of any excitation light source is the inherent advantage of CL detection, which not only eliminates the problematic background emission from interfering compounds or from the microfluidic substrate itself. CL is also more appropriate for miniaturization of the on-line detection system and to build a portable microfluidic instrument [64, 65]. Thus, CL is a promising alternative detection technique to be coupled to microfluidic analysis for a miniaturized device. However, CL is limited to some special reaction reagents, such as luminol and its derivatives [66], peroxyalate and oxalate [64], and ruthenium complexes and to direct oxidations [65]. Till now, CL detection coupled to capillary electrophoresis has been well reviewed [67–70]. Herein, we briefly introduce recent developments in the use of CL on microchips.

In 1998, CL detection coupled to microfluidic was first described by Mangru and Harrison [66]. Based on horseradish peroxidase (HRP)-catalyzed reaction of luminol with peroxide, they designed a postseparation detection scheme on a microchip by transporting peroxide into the separation channel from a bypass channel. A 7 nM detection limit for the fluorescein conjugate of HRP was achieved. To optimize the microchip layout and reaction conditions for different CL reagents, Liu et al. [71] compared two chip layouts (cross-combining with Y, and cross-combining with V) in PDMS and evaluated their performance with respect to two model CL systems that included the metal-ion-catalyzed luminol–peroxide reaction and the dansyl species conjugated peroxyalate–peroxide reaction. A comparison between these chip layouts showed that the chip pattern of cross-combining with Y may be more promising for the luminol–peroxide CL system, while the chip pattern of cross-combining with V was preferred for the peroxyalate–peroxide system.

Hashimoto et al. [64] simplified the chip layout without etching the manifolds. The detection point was set at the interface of separation channel and reaction reservoir. They successfully separated and detected dansyl amino acids (glycine and glycine) using peroxyoxalate CL reaction using CL detection-based microchip capillary electrophoresis. They further incorporated an immune reaction with CL detection to determine human serum albumin or immunosuppressive acidic protein as a cancer marker in human serum [72].

After CL detection was successfully introduced to the microchip and optimal channel design and reaction conditions were obtained, it was used for high-sensitivity detection, especially for single cells analysis. Zhao et al. [73] first reported that CL detection with microchip electrophoresis was used to determine the intracellular content of glutathione in single human red blood cells. CL detection showed about 100 times more sensitivity than LIF detection for single cell analysis.

The same group subsequently quantified Gly and Ala in single rat hepatocytes cells [74], taurine and amino acids in mice single fibrosarcoma cells [75], and sulfhydryl compounds in single red blood cells [76]. They further developed a CL resonance energy transfer method to detect the amino acids in single human red blood cells [77]. Besides intracellular content analysis, the counting of intact cells by CL detection on microfluidic chip was designed by Wang et al. [78]. They counted CD4-positive ($CD4^+$) T-cells from whole blood by capturing $CD4^+$ T-cells with anti-CD4 antibody. The trapped cells were then bound to CD3 antibodies conjugated with HRP and incubated with chemiluminescent substrate. The emitted photons were proportional to the number of captured $CD4^+$ T-cells. The results can be provided automatically and digitally within seconds of running the test. Chemiluminescence detection on the microfluidic chip provides the highest potential to reduce the size of instruments compared with other optical detection systems due to the lack of an external light source, which makes it possible to produce low-cost point-of-care diagnosis microdevices. However, the crucial drawback of CL detection in microfluidics is its poor reproducibility because CL measurements are strongly affected by many factors, including temperature, pH, solvent, solution composition, etc. Furthermore, the number of CL reagents is limited.

2.4 Surface Plasmon Resonance and Localized Surface Plasmon Resonance

Surface plasmon resonance (SPR) is an optical method for probing the refractive index changes of medium (sample) in contact with the surface of a noble metal film in which coherent electron oscillations result in resonance. SPR is a particularly suitable technique for measuring rates and equilibrium constants of processes that involve molecular interactions and adsorption of biomacromolecules on surfaces. A light wave is coupled to the metal film to excite the surface plasmons. If analytes bind to the metal film surface, a change in the refractive index of the medium alters the characteristics of the light wave coupled to the surface plasmon. Measuring the alteration of the excitation light reflects the species and concentrations of the analytes. The basic principles, couplers and applications of SPR have been well documented by Homola [79]. An SPR spectroscope usually incorporates a flow cell to confine and control the sample flowing through the sensing surface. Microfluidic chips provide an easy manner for sensing very small amounts of samples without an optical tag when SPR or localized surface plasmon resonance (LSPR) is integrated onto microchips.

Coupling SPR to microfluidic systems is usually implemented by prism, waveguide, and metal grating. In the prism coupling mode, the walls of microfluidic channels are deposited with a layer of gold film for sensing the change of analytes flowing through the film [80–82]. The excited light is totally internally reflected by the prism, which is in contact with the metal film, and is introduced to the metal film through evanescent wave. Figure 5a shows a schematic of prism-coupled SPR for a microfluidic chip. This traditional coupling approach is simple, sensitive, and

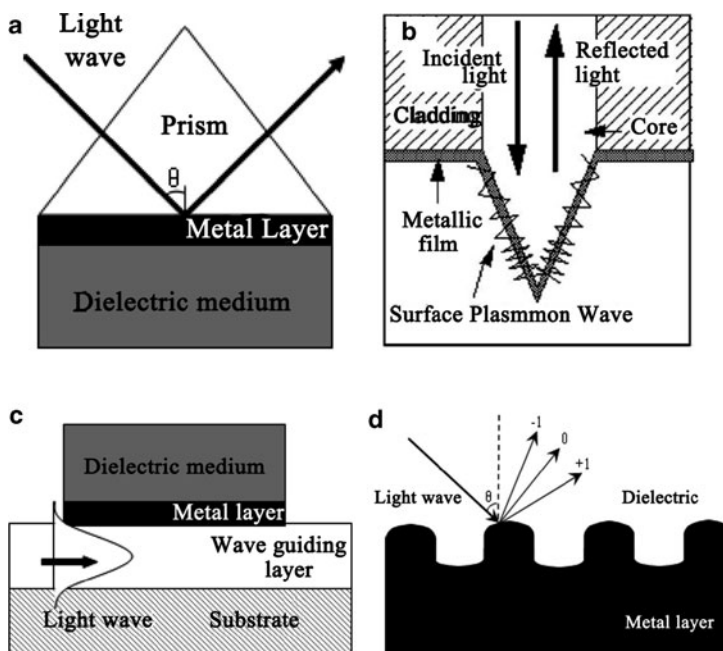


Fig. 5 Coupling schemes of incident light to surface plasmons: (a) prism coupling, (b) experimental setup for the fiber-optic SPR microsensor, (c) waveguide coupling (Reprinted from [83] with permission of Elsevier), and (d) grating coupling

robust, but it is less advantageous in miniaturization and integration. Optical fibers and waveguide have been developed as alternatives to the prism to generate evanescent waves and to excite the surface plasmon. Kurihara etched a fiber to form a gold-coated microtip at the end of the fiber and inserted it into a micro-channel [83]. The coated microtip has features like a microprism (Fig. 5b). Fiber-based SPR on-chip has the problem of alignment and assembly. To overcome such issues, it was proposed that the planar optical waveguide coupling mode should be integrated on the microfluidic chip (Fig. 5c) [84, 85]. The waveguide-based SPR on-chip has the potential of high throughput analysis of multiple samples in parallel because multiple waveguide structures can be fabricated into one single platform. Another promising alternative method for the miniaturization is SPR-based grating, which is low-cost and can be mass-produced by disposable polymer materials instead of the glass chip used for prism or waveguide SPR [86, 87]. In this coupling mode, a metal grating profile coated on the channel diffracts the incident light wave, which is capable of matching the momentum of the plasmon and the wave and generating a surface plasmon (Fig. 5d). In this approach, noncontact optical excitation obviates the need for a prism and index-matching fluids and greatly simplifies instrument configuration.

The excitation of surface plasmons that occurs at the planar surfaces is denoted as SPR; that which occurs at the surface of nanometer-sized metallic structures is

called LSPR. SPR-based systems require coating of metal film on the walls of the microchannel and finding an appropriate way to couple the light to the surface plasmon. However, LSPR merely requires the immobilization of metal nanoparticles in the channel [88], which substantially reduces the fabrication cost and the optical setup complexity. LSPR seems to be sensitive enough on the microfluidic chip because Cao et al. have measured the changes in the LSPR signal of a single Au nanoparticle by dark field microscopy [89].

2.5 Surface Enhanced Raman Spectroscopy/Imaging

Surface enhanced Raman spectroscopy (SERS) occurring on the surfaces of noble metal substrates or nanoparticles and is another highly sensitive detection method based on surface plasmon, without requiring labeling. In contrast to conventional Raman spectroscopy, the detection sensitivity of SERS is enhanced up to 6–10 orders of magnitude. The advantages of SERS detection on microfluidic chips are expected to yield reliable and reproducible results and to obtain precise quantitative measurement because the experimental conditions in the microchannel are easier to control than that of bulk SERS, which has been discussed in a review of chip-based SERS published in 2008 [90]. Besides probing the fingerprint of molecules, a SERS-coupled microfluidic device has been used for characterization of single Chinese hamster ovary cells, into which gold nanoparticles were introduced for Raman enhancement [91]. Herein, we only focus on progress published after 2007 and in which metal nanoparticles were exploited as the SERS enhancer.

The targets of present SERS on-chip are (1) to solve the problem of poor detection sensitivity caused by the small sample volume and (2) to develop robust methods to obtain a reliable and reproducible SERS signal. Aggregation of metal nanoparticles and mixing of enhancer with analytes are the straightforward ways to increase the SERS signal intensity and the uniformity of the SERS active site.

In general, SERS signal intensity is related to the number of molecules, Raman cross-section and the enhancement factors. Among these parameters, molecular quantity is the only controllable variable for the signal enhancement at given experimental conditions. Therefore, increasing the amount of absorbed molecules in the detection area can amplify the SERS signal. Various ways have been proposed for accumulating nanoparticles in microdevices and three are listed below:

1. Hampering nanoparticles by a dam or restricting them in reservoir: Choi et al. [92] concentrated rhodamine 6G-adsorbed gold nanoparticles by repeating a “filling–drying” cycle on a (compact disk) CD-based platform. They readily achieved a SERS signal of 1 nM rhodamine 6G. Wang et al. [93] developed a pinched and step microfluidic–nanochannel junction like an inverted dam, where nanoparticles and target molecules were stopped and assembled, and obtained electromagnetic enhancement factor of $\sim 10^8$. This technique was also used for monitoring the conformational transition of beta-amyloid peptide [94].

2. Use of electrokinetic force: Huh et al. [95] embedded microwells in a microchannel, the top and bottom of which were fabricated with a pair of electrodes. When electrically actuated, gold nanoparticles bound with DNA molecules were attracted into the microwells by the electric field, and the sensitivity of SERS was significantly increased. The authors reported the detection limit of 30 pM for Dengue sequences. Similarly, Cho et al. [96] reported accumulation of electrokinetically driven charge molecules on an Au surface and amplified the SERS signal by almost eight orders of magnitude.
3. Coupling a laser tweezer to a microdevice for aggregating metal nanoparticles: When nanoparticles flowed through focused red laser beam, they were trapped by the laser beam and assembled together. Another green laser was used for SERS excitation. Although the instrument was complex, it provided potential for controllable aggregation of nanoparticles and sequential analysis of samples in one run [97]. Based on above advances, we will not be surprised if magnetic force will be used for trapping metal enhancer in the near future.

SERS detection is restricted in quantitative analysis due to its poor reproducible results. A consistent and homogeneous mixing between the analytes and nanoparticles before they arrive the detection point is helpful in improving reproducibility. Therefore, various shapes of microchannels have been designed to increase the mixing effect, such as alligator-teeth, zigzag, 3D channel, etc [90]. Recently, Quang et al. [98] fabricated a pillar array in a PDMS microfluidic channel to efficiently mix sample and enhancer. Two confluent streams of analytes and silver nanocolloids were introduced into the pillar array channel and then the SERS spectra were recorded at the downstream end of the channel. Using this pillar array channel-based SERS, they achieved the quantitative analysis of dipicolinic acid and malachite green, and the detection limits were estimated to be 200 and 500 ppb, respectively.

3 Detection Inside the Chip

Optical detection inside the chip means that optical detection relevant units, such as light sources, filters, mirrors, waveguides, lenses, and detectors, are integrated on the chip. Those microfluidic chips integrated with optical components that are merged with or made of fluids are also called “optofluidic.” It is obvious that the more functional units, including optical components, are integrated on the chip, the degree of miniaturization of the microdevice is higher. Compared with free-space optics systems, the integrated optical microfluidic system is alignment-free and technician-independent [99]. Since such integrated microsystem is compact and firm, it is insensitive to shock and vibration, and can be used under extreme environments. In addition, if the light is well guided inside the chip, it can minimize light loss and the emergence of stray light as much as possible, increase the utilization efficiency of probing light, and decrease the background. Most current

progress on detection inside a chip is concentrated on developing various strategies for assembly of optical elements on the chip. For example, previous reviews have discussed the structure and fabrication of the optofluidic waveguide [100], optofluidic microlens [101], microscope on-chip [102] and so on. With the advance of manufacturing technologies, integrated optical devices in the near future would be less expensive, with response times much faster than ever before. The full integration of optical elements into microfluidic chip is becoming possible.

3.1 Planar Optical Waveguide

Optical waveguide is a physical structure that transmits light along its axis, which is generally composed of “core/cladding.” A planar optical waveguide is a waveguide fabricated in a flat platform, and herein refers particularly to microfluidic chip. A waveguide is a key optical element for integrated optofluidics, and has the same importance as the fluidic channel in directing fluids. When the optical waveguide and the fluidic guide are merged together, the degree of integration is maximum. In microfluidic systems, planar waveguides have been used to enhance the detection sensitivity, such as focusing the light to the channel to increase the excitation power for fluorescence measurements [103], extending the optical path length in absorbance detection [104], and splitting the laser beam for interferometry sensing [105, 106]. The current status is that two types of waveguides have been assembled on microchips. One type is based on the refractive index, whereby the light is confined in the core material by total internal reflection because the core has a higher refractive index than that of the cladding. There is an electric field in the cladding layer, which typically penetrates 100–200 nm depths and decays exponentially outside the core. This field is called the evanescent wave. The other type of waveguide is the interference-based waveguide, in which the light is reflected back to the core by interference rather than internal reflection; therefore, the refractive index of the core need not be larger than that of the cladding.

3.1.1 Evanescent Wave-Based Waveguide

Depending on the materials used for core and cladding, waveguides based on total internal reflection are divided into three types: solid-state waveguides, liquid-core waveguides (LCWs), and liquid-core/liquid-cladding (L^2) waveguides.

Solid-state waveguides are usually buried in the chip and intersect the fluidic channel to excite the analytes and collect the response signal. Solid-state waveguides are fabricated with the same materials as the chip, such as silica, glass and polymer. Silica and glass have the advantages over polymer materials of being chemically inert, biocompatible, and optically clear, and are usually used for improving sensitivity in absorption and fluorescence detection. Petersen et al. buried a doped silica waveguide on microfluidic separation devices for UV/Vis

absorbance measurements [20]. A ninefold higher sensitivity was achieved with this approach compared to a conventional CE instrument with a 75- μm inner diameter capillary. The authors further fabricated 128 waveguides on-chip for multipoint detection to measure particle velocities [107]. Cleary et al. fabricated a silica waveguide on a chip and realized time-correlated single-photon counting of Nile blue with concentrations as low as 1.5 nM [108].

However, glass and silica materials suffer from fabrication and mass production difficulties due to their complex processing technology and high cost. A variety of recent developments in assembling waveguides on microdevices have concentrated on polymer materials such as PDMS [109, 110] and poly(methyl methacrylate) (PMMA) [111] for large-scale production and cost reduction. Very recently, Okagbare et al. [112] developed a cyclic olefin copolymer waveguide embedded in a PMMA fluidic chip. The evanescent wave outside the cyclic olefin copolymer waveguide was used to simultaneously excite fluorophores in 11 fluidic channels for high-throughput analyses. The limit of detection for an Alexa Fluor 647 dye solution was 7.1×10^{-20} mol at a signal-to-noise ratio of 2.

The solid state waveguide is assembled into the microchip but separately fabricated with the microchannels. The connection point of fluidic channel and solid waveguide is generally the interrogation area. However, LCWs share the same physical volume with the fluidic channel. The microchannel not only transports the sample, but also transmits the light, which greatly simplifies the design complexity and reduces light loss through the channel walls. If liquid (particularly water in a microfluidic chip, with refractive index of 1.33) is used as the core of waveguide, the refractive indices of the cladding should be smaller than that of water, based on the principle of total internal reflection. Teflon amorphous fluoropolymers (Teflon AF) with an indices of 1.29–1.31 is a suitable cladding material for a LCW in a microfluidic chip. Datta et al. [113, 114] coated Teflon AF on silicon and glass substrate as cladding layer, and fabricated the coated substrates into microchannels that were also LCWs to propagate light. Detection of nanomolar concentrations of fluorescent dye was achieved on the liquid-core waveguide integrated chips. In order to reduce the time-consuming and high-cost fabrication processes using glass and silica substrates, Wu et al. [115] coated Teflon on the PDMS substrate and assembled a liquid-core waveguide on a PDMS/glass hybrid microfluidic chip to sense nitrite. Cho et al. [116] developed a method to construct LCWs in PDMS microchannels by flowing Teflon AF solution through the channels. This coating approach avoids the difficulties of bonding between two Teflon-coated PDMS substrates [115]. A micro fluorescence-activated cell sorter in the Teflon-coated LCW was further demonstrated. The laser was introduced into the microchannel, i.e., the LCW, from its one end and the prestained cells in microchannel were all excited. Therefore, the cells can be sorted into a split channel at the downstream side [117]. Replacing a commercialized Teflon tube with a fabricated liquid core in channel is an alternative method for improving sensitivity in a microdevice. For example, Du et al. [118] coupled a Teflon AF capillary to the chip channel as the detection cell for microchip absorption detection and achieved an effective optical path length of 17.4 mm with a detection volume of only 90 nL. In 2010, Pan et al.

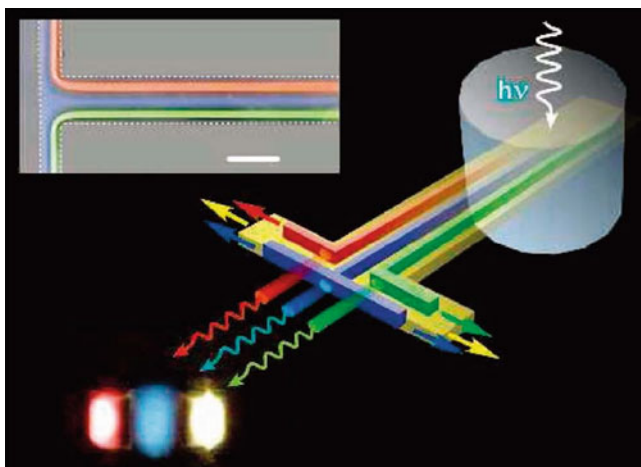


Fig. 6 Three parallel waveguides formed with liquid core and cladding in laminar flow systems. The direction of the light propagation can be altered by different flow rates of the adjacent fluids. $h\nu$ refers to the energy of light; h is the Plank's constant; ν is the frequency of the light. (Reprinted from [121] with permission of The American Chemistry Society)

[27] integrated Teflon LCWs, photometer, LEDs and other components into a hand-held instrument. Teflon has long been the only option for low refractive index cladding for LCWs until nanoporous dielectrics were developed. Nanoporous materials are formed with a high-index solid material by adding air pores, therefore the refractive index can be adjusted by varying the air fraction. At the same time, the wall of nanoporous cladding can be chemically functionalized, overcoming some of the adhesion problems of Teflon [119]. Korampally et al. fabricated nanoporous film of low refractive index on the silicon microchannel and developed a miniaturized LCW [120].

L^2 waveguides are formed by two or more different laminar liquids of different refractive index flowing inside a fluidic channel. The index of the cladding liquid is smaller than that of the core liquid so that the light is guided in the channel by the total internal reflection that occurred at the interface of the liquids. By changing the flow rates of the liquids, the size and the direction of the waveguides can be reconstructed (Fig. 6) [121, 122]. The advantages of L^2 waveguides over solid-state waveguide are: (1) the optical performance is tunable by controlling the fluidic properties; and (2) the smooth interfaces between the core and cladding streams minimize optical loss. To couple an L^2 waveguide with a biosensor, Rosenauer et al. [123] fabricated a liquid-core/liquid-twin-cladding waveguide for on-chip fluorescence spectroscopy. The design included an inner and an outer cladding fluid outside of the core fluid; analyte was suspended in the inner cladding fluid and excited by the evanescent wave at the fluid interface of core and inner cladding. By tuning the flow rate ratios of the three different liquids, considerable reduction in sample volume and a low background noise were achieved. The detection limit of rhodamine B dye was 20 μM . The L^2 waveguide in a 2D plane suffers from optical

loss at the top and bottom interfaces of core and channel walls. Lee et al. [124] therefore developed a 3D microfluidic L^2 waveguide by using microfluidic drifting technology [125], where the liquid core cannot come in contact with the channel walls because it is hydrodynamically focused in the center of the microchannel by the cladding fluids. In addition, the laminar flow-based L^2 configuration has been widely applied to construct other optical components, such as reconfigurable lenses [126], optical switches [127], and tunable micro-optofluidic prisms [128]. Although current L^2 waveguides may be restricted by the sensitivity of the stream interface to vibrations and diffusion effects, and limited on finding liquids with specific refractive indexes, the tunability of L^2 waveguides makes it possible to provide functionality and integration in future optofluidic devices.

3.1.2 Interference-Based Waveguide

The interference-based waveguide is a conceptually different approach for realizing LCWs in microfluidic chips. In contrast to the evanescent wave-based waveguides, interference-based waveguides do not require a cladding material with a lower index than that of the core material. Light is multiply reflected from a periodic dielectric cladding layer by wave interference. There are two types of interference-based waveguides: photonic crystal (PC) waveguides and antiresonant reflecting optical waveguides (ARROWs).

The integration of PC fibers on glass chip has been demonstrated by means of femtosecond laser exposure and chemical etching [129]. However, so far no microfabricated PC-based LCW has been reported. ARROWs have attracted more attention from researchers in the microfluidic chip field due to their relatively easy fabrication from accessible materials using current micro-electromechanical techniques. The main feature of ARROWs is that light is confined by Fabry–Perot antiresonant reflectors, rather than total internal reflection. Therefore, ARROWs can be constructed in a low refractive index core, such as an aqueous solution, surrounded by high refractive index cladding layer such as a silicon substrate. Planar integrated networks of intersecting solid and LCWs on a chip were used for single dye molecule detection [130] and single liposome particle detection [131]. Further information about integrated waveguiding can be found in reviews by Schmidt et al. [100, 132].

3.2 Microlens

The microlens is an important and key optical component for focusing and collimating light in the microfluidic optical detection system, and can be made up of a hard solid surface or interface (soft solid/liquid, liquid/liquid/. . .). Hard solid state lenses on-chip are usually fixed focal length lenses similar to the miniaturized traditional lenses used in the free-space detection system. They can be fabricated

on-chip with the optical axial vertical to the chip plane, focusing light to the channel from top or bottom surface [133], as well as with optical axis parallel to the plane, introducing light from the side wall of the chip [25, 134]. Although solid lenses suffer from the complexity of fabrication and alignment, they are robust and vibration resistant. Recently, such microlenses have been fabricated on a SU-8/PDMS hybrid microfluidic chip for optical manipulation of microparticles [135]. Other promising and popular microlenses on-chip utilize the curvature formed by the interface between two liquids, between liquid and soft solid, or between liquid and air. Such microlenses are also called optofluidic microlens, and they are dynamic optical elements and their focal lengths can be easily tuned by changing fluid characteristics such as species, concentration, and flow rate. Next we will focus the discussion on optofluidic microlenses.

The major advantages of these interface-based microlenses are that they are reconfigurable and optically smooth meniscus surfaces. Light can be modulated by simple adjustment of the flow conditions, thus eliminating the need for mechanical or electrical parts for manipulating the lens on the microchip.

Elastic PDMS is a commonly used polymer material for fabricating microfluidic chip and because it is readily curved by air pressure or liquid hydrodynamic, it has been used to shape a curvature and form a microlens by deforming with pneumatic force. For example, a PDMS wall with a thickness of 50 μm between chambers and microchannel can be distorted by applying liquid pressures flowing through chambers. The deformation of the PDMS wall and the index-matching fluid act as a double convex lens to focus both the excitation light source and the fluorescent emission signal. The focal length can be adjusted through different liquid pressures [136]. Changing the curvature of the PDMS surface can also be realized out-of-plane by exerting electrical force [137] and electromagnetic force [138]. However, the distortion of the surface is limited, and a large curvature of the PDMS surface is hard to form by external force. To address this issue, Shi et al. [139] fabricated a tunable in-plane optofluidic microlens set involving a static PDMS lens and an air–water interface that diverged the light and was reshaped by adjusting the flow rate of the injected water. The tunable divergence in the incident light beam, in turn tuning the overall focal length of the microlens, was converged by the static PDMS lens. The microlens achieved tunable focal distance of 11 mm and a ninefold light intensity enhancement at the focal point. In addition, the liquid–liquid interface promises another way of forming a large curvature microlens.

Liquid–liquid microlenses were generated for the first time on-chip by Mao et al. [140]. Subsequently, Rosenauer et al. designed a hydrodynamically adjustable convex lens with 3D light focusing ability instead of line focusing [141] (Fig. 7). The authors co-injected miscible fluids of different refractive indices and formed the interface in the channel. When the liquids flow through a 90° curve in a microchannel, a centrifugal effect also curves the fluidic interface and yields a reliable cylindrical microlens. The curvature of the fluidic interface can be altered by simply changing the flow rate. Higher flow rates generate a microlens with larger curvature and, hence shorter focal length. Tang et al. [142] reported another L^2 lens formed by laminar flow of three streams of fluids (Fig. 8). The refractive index of

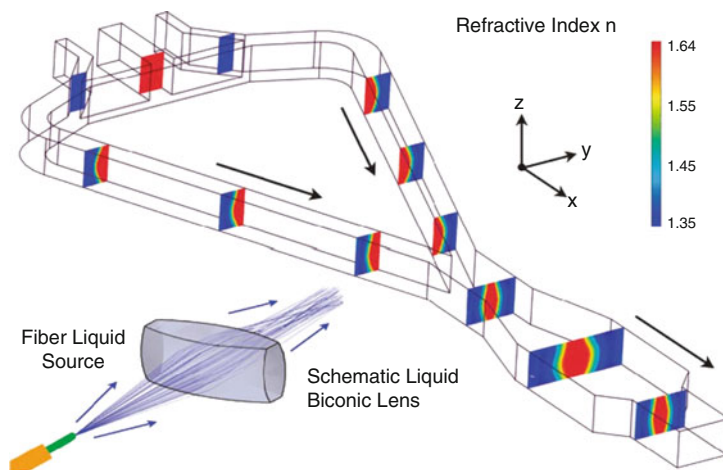


Fig. 7 A 3D light-focusing optofluidic microlens. The displayed cross-sections show the shaping of the lens and the refractive index step defined by the choice of core and cladding fluids (Reprinted from [141] with permission of The Royal Society of Chemistry)

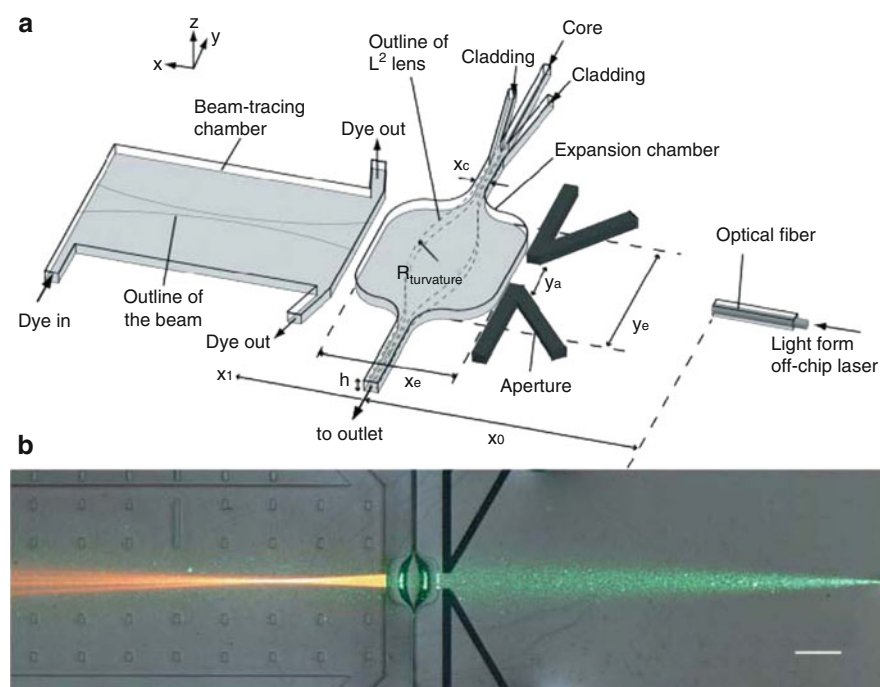


Fig. 8 (a) Experimental setup for focusing light exiting an optical fiber through the liquid-core/liquid-cladding (L^2) lens. (b) Bright-field image of the L^2 lens. The *green* laser beam from the fiber is visible in front of the aperture because PDMS contains nanoparticles of silica that scatter light. The focused beam in the beam-tracing chamber is *orange* due to the fluorescence of the dye. (Reprinted from [142] with permission of The Royal Society of Chemistry)

the central (core) stream was higher than that of the sandwiching (cladding) streams. When the streams entered an expansion chamber, the lens was formed. The curvature of the interface between the liquid core and the liquid cladding can be modulated by adjusting the relative flow rates, resulting in variable focal distance. As a result of the change of the expansion chamber to a circular chamber, interfaces with a perfect arc shape and a short focal length can be obtained [143, 144]. However, diffusion of solute across the fluid–fluid interface deteriorates the smoothness of the interface. Therefore, Huang’s group developed in-plane [126] and out-of-plane [145] lenses on the microchip that were dependent on the liquid gradient refractive index (L-GRIN), and focus light due to the gradient of the refractive index within the liquid medium, rather than due to curved refractive interfaces (Fig. 9).

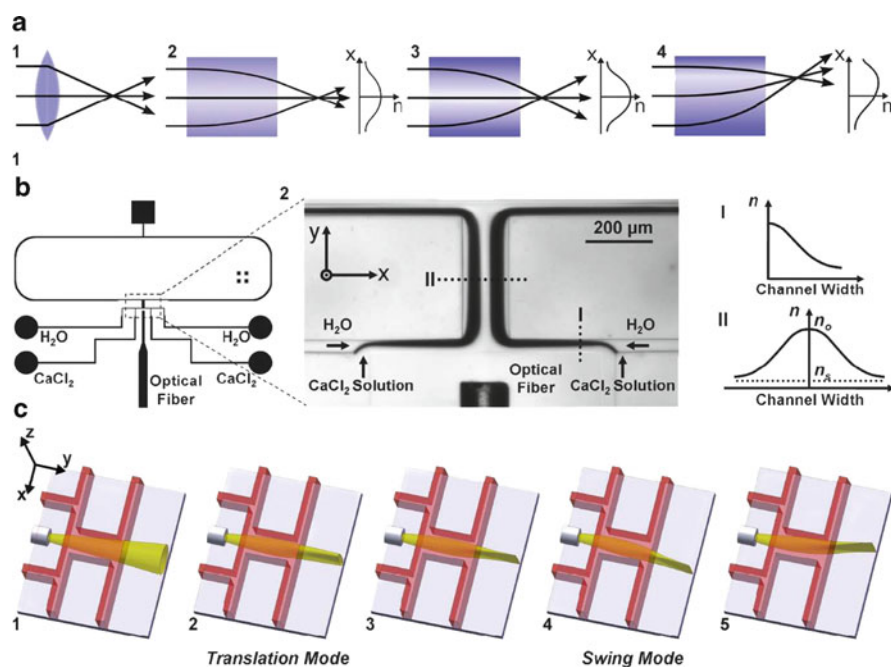


Fig. 9 Principle and design of the L-GRIN lens. (a) Comparison between the classic refractive lens (a1) and GRIN lens (a2). Change of the refractive index contrast in GRIN lens can result in change of focal distance (a2, a3), and shift of optical axis can result in change of output light direction (a4). (b) Schematic of the L-GRIN lens design (b1), microscopic image of the L-GRIN lens in operation (b2, left), refractive index distribution at two locations (b2, right) (c) Drawings showing two operation modes of the L-GRIN lens: the translation mode with variable focal length including no-focusing (c1), a large focal distance (c2), and a small focal distance (c3); and the swing mode with variable output light direction (c3–c5) (Reprinted from [126] with permission of The Royal Society of Chemistry)

3.3 *Optofluidic Laser*

To achieve the ultimate goal of integration of many optical components onto a compact chip, laser integration on-chip is a key challenge, although conventional bulky lasers have been widely applied in microfluidic systems through free-space coupling [7, 8]. The miniaturized laser had been independently developed before the microfluidic chip was put forth. However, only when the microfluidic device and microphotonic system are synergetically combined, can the optofluidic chip be successful. Therefore, we will not attempt to discuss light sources that are miniaturized and assembled on the microchip but have nothing to do with fluids, although they have made contributions to the development of laser miniaturization. For example, the laser diode, photodetector, and waveguide have all been integrated on a silicon chip [146], as well as an organic semiconductor film laser assembly on a PMMA substrate [147]. The dye laser is currently the optofluidic laser most usually integrated on microfluidic chips [148]. The advantages of optofluidic dye lasers are that they can be fabricated on the same materials as the microfluidic system and readily integrated with other fluidic functionalities, and that the characteristics of dye lasers are amenable to tuning by changing the dye solution. Since the first optofluidic dye laser was reported in 2003 [149], rapid and significant progress has been obtained in terms of various configurations and materials. Lasers consists of three principal elements: gain medium, pump source, and resonator cavity. Since the pump sources for the present optofluidic dye laser are all external light sources such as lasers, and the gain mediums are various dyes in different solvents, both of which are less related to chip structure, we will summarize the development of optofluidic lasers with respect to the resonator, which is an optical feedback volume that repeatedly transmits a resonant light through the gain medium to create a very intense, coherent laser. This optical feedback system is conventionally called the optical resonator or optical cavity.

The simplest optical cavity comprises only two facing plane mirrors, denoted as a Fabry–Perot cavity. Helbo et al. [149] first deposited a pair of opposing metal mirrors on the top and bottom of a microchannel acting as a resonator in which rhodamine 6G solution flew through as the gain medium (Fig. 10). Song and Psaltis have recently developed a pneumatically tunable optofluidic dye laser [150], in which a LCW filled with dye solution is the resonator at the ends of which two air chambers act as the mirrors. The wavelength is chosen by inflating the air-gap etalon with compressed air.

A ring resonator is the second simple configuration for a cavity consisting of three or more mirrors to loop the light in the resonator. Galas et al. fabricated a ring resonator using four mirrors (air chamber) to generate a tunable dye laser [151]. Suter et al. [152] presented side-coupled ring geometry to generate an optofluidic ring resonator laser, which can be produced in PDMS substrates with contact molding (Fig. 11). A kind of variation of the ring cavity structures is the droplet-based whispering gallery mode. A droplet can be treated as an optical microcavity when the index of refraction of enclosed dye solution is higher than that of

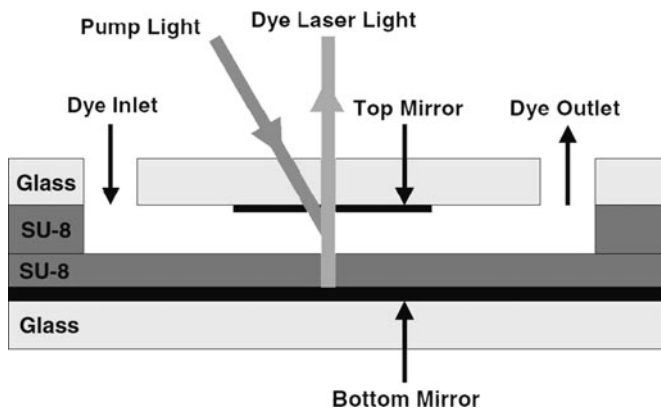
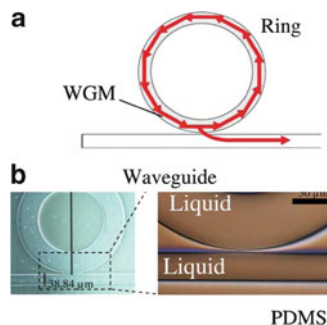


Fig. 10 Cross-sectional outline of the microcavity fluidic dye laser. The laser dye is pumped through a microfluidic channel. The laser cavity is formed inside the microfluidic channel by metal mirrors, deposited on the top and bottom glass wafers. The microcavity fluidic dye laser is pumped by an external laser, and output is emitted through the semitransparent top mirror (Reprinted from [149] with permission of IOP Publishing)

Fig. 11 (a) Cross-sectional outline of the microcavity fluidic dye laser; *WGM* whispering gallery mode. (b) Photograph of a glass/SU-8 chip with a microcavity fluidic dye laser (Reprinted from [152] with permission of The Optical Society of America)



the carrier liquid. Light emitting from the dyes is confined and amplified in the drops by total internal reflection. This method could provide a multicolor laser in a train of alternating dye drops and is capable of switching the wavelength at high frequency [153].

Besides the mirror-based optical cavity, there is another type of optical feedback structure involving diffraction grating, called distributed feedback (DFB). The group of Kristensen demonstrated a 130th order Bragg grating-based optofluidic dye laser [154] to achieve a single mode laser. However, lower-order DFB gratings are expected to minimize the intrinsic scattering losses and decrease the threshold of pump energies. Therefore, the 15th order [155] and third order [156] Bragg gratings were successively fabricated on a microfluidic chip. Song et al. [157] have systematically studied third, second, and first order DFB lasers, where the second order lasers exhibited the lowest pump threshold. Vannahme et al. [158] embedded a first order DFB optofluidic dye laser in a foil for mass production and cost reduction.

At least two issues should be improved to fulfill the promise of optofluidic dye lasers as on-chip coherent light sources. Firstly, new strategies should be developed to widen the laser wavelength range and to reduce the tuning time. Secondly, the optical pump source should be integrated onto the same laser chip, which should demonstrate the lowest laser threshold.

3.4 *Optical Detector*

Optical detectors have been integrated on microfluidic chips, such as silicon photodiode, organic photodiodes (OPDs), and complementary metal–oxide–semiconductor (CMOS) chips. The former two are point detectors without spatial resolution, whereas CMOS detectors can capture an image. In the early stage, integrated detectors on microfluidic chips were mainly silicon detectors due to the mature fabrication technique of semiconductors, e.g., a microavalanche photodiode on PDMS [159], a photodiode built on a silicon substrate [160], and a hydrogenated amorphous silicon photodiode assembly on glass [161]. Generally speaking, the fabrication procedure for a detector on-chip becomes less and less complex, and the cost of detector trends to become lower and lower. For example, if the substrates are changed from silicon to glass and then to polymer, the fabrication temperature is decreased from a high temperature to ambient temperature. Recently, Pereira et al. presented an example by integrating a PIN photodiode on a microfluidic chip to perform chemiluminescent detection, and the detection results were comparable with laboratory analysis for detection of HRP [162].

Silicon photodiodes could render relatively high sensitivity for detection of low analyte concentrations but are too expensive and complicated to fabricate as an integral part of a disposable microfluidic chip. In contrast to the silicon counterpart, OPDs are a promising potential for future point-of-care technology because they are inexpensive and easily fabricated, and are attracting more and more attention from researchers in the field of lab-on-chip.

Hofmann et al. [163] showed the feasibility of integration of thin-film OPDs on microchips for microscale chemiluminescence. The detector was fabricated by a layer-by-layer vacuum deposition method. The quantitation of hydrogen peroxide yielded a detection limit of 1 mM. They further implemented the integration of OPD on PDMS instead of silicon as the substrate material [164] and applied it to analyze antioxidant capacity [165]. To reduce the background and increase the detection limit of the OPD detector on chips, Pais [166] placed a second polarizer layer before fluorescence entered into the OPD detector by preventing the leaking of excitation light into the detector. The detectable concentrations of rhodamine 6 G and fluorescein dyes were as low as 100 nM and 10 μ M, respectively. Wojciechowski et al. [167] developed a chemiluminescence immunoassay-based miniaturized biosensor, which was composed of a disposable microscope slide and a hand-held reader. The OPD substrate was printed on the glass slide. This OPD

system is approaching the final requirements of point-of-care, i.e., inexpensive, easy to use, highly sensitive, and robust.

Besides the various photodiodes mentioned above integrated on microfluidic chips, the CMOS is another type of detector that can be assembled on microchips and offers the great advantage of the ability to observe the image of sample object [63]. One of the most important applications of an integrated CMOS detector on-chip is the lensless optofluidic microscopy (OFM). In 2005, Lange et al. [168] attached a CMOS chip at the bottom of a microfluidic chip to record the projection image of *Caenorhabditis elegans*. But, the quality of this imaging method needs to be further improved by choosing appropriate apertures. Yang et al. [169, 170] were inspired to develop a high-resolution optofluidic microscope by covering a nanohole array layer on the imaging chip. They measured a resolution limit of 490 ± 40 nm, comparable resolution to a conventional microscope. The principle of lensless microscopy is shown in Fig. 12. The authors extended this method to color OFM by integrating a RGB CMOS color sensor chip substrate [171]. Laurberg et al. then exploited OFM to 3D spatial resolution and on-chip particle image velocimetry [172].

Yang's group further presented a non-nanohole method for reconstruction of a high-resolution image from a low-resolution image processed with a pixel super-resolution algorithm [173]. This method further compacts the OFM by eliminating the nanoaperture array, and follows the consistent requirement of

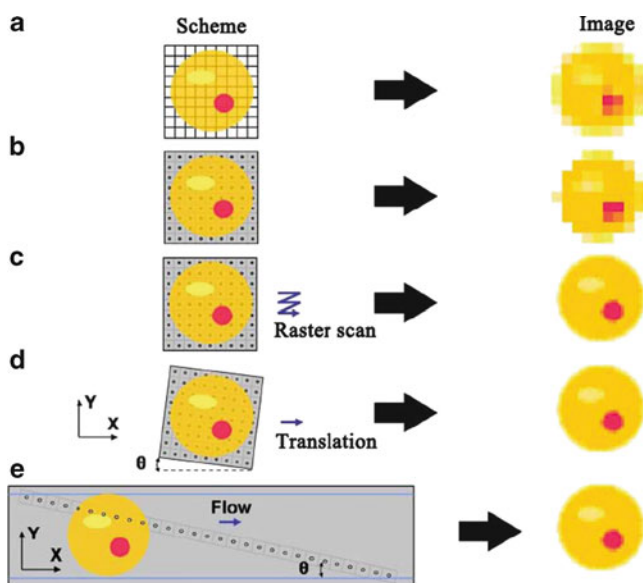


Fig. 12 Principles of nanohole microscopy. (a) Direct projection imaging scheme. (b) By placing the specimen on a grid of apertures, we can obtain a sparse image. (c) Raster-scanning the specimen over the aperture grid. In this case, the image resolution is limited by the aperture size. (d) The scanning scheme can be simplified into a single-pass flow of the specimen across the grid. (e) The aperture grid can be simplified by substitution with a long linear aperture array (Reprinted from [170] with permission of The National Academy of Science, USA)

microfluidic chip in miniaturization as small as possible. The rapid development of OFM is following the advances in optofluidics but also contributes to them.

4 Conclusions

Optical detection still maintains its predominant application in microfluidics due to its characteristics of being noninvasive, easily coupled, quick to respond, and highly sensitive. As discussed, although conventional free-space detection strategy is less amenable to being miniaturized and compacted in a portable microdevice, it is highly familiar to analytical chemists, and is still helpful when a proof-of-principle needs to be quickly demonstrated on microfluidic chips and extreme sensitivity is a particular concern. As the most promising alternative to free-space detection, optofluidics is becoming an active field in lab-on-a-chip, merging fluidics with optics in the same microchip, in which optics are generated by fluids and fluids are controlled by optics. Current optofluidics is developing and optimizing single optics, but has potential to minimize and integrate all components onto the same microscale device, which includes analytical units and optical pieces. In optofluidics, various optical components such as light source, filters, microlens, detectors, and waveguides can be made of fluids; therefore, the space in the chip is greatly saved and the complexity of fabrication is simplified. The microchannel both handles the analytes and transmits light to probe the sample and collect analytical results. Future optofluidic chips undoubtedly can integrate more components and be mass-produced to meet the requirements of point-of-care diagnostics.

Acknowledgments The authors would like to thank Xingbo Shi, Xinliang Liu, Lichun Sun, and Haixia Ding for helpful discussions. HWG gratefully acknowledges the support of National Natural Science Foundation of China (20705007, 21075033, 20703016).

References

1. Manz A, Fettinger JC, Verpoorte E, Ludi H, Widmer HM, Harrison DJ (1991) *TrAC Trends Anal Chem* 10:144–149
2. Einav S, Gerber D, Bryson PD, Sklan EH, Elazar M, Maerkl SJ, Glenn JS, Quake SR (2008) *Nat Biotechnol* 26:1019–1027
3. Walsh CL, Babin BM, Kasinskas RW, Foster JA, McGarry MJ, Forbes NS (2009) *Lab Chip* 9:545–554
4. Gerber D, Maerkl SJ, Quake SR (2009) *Nat Methods* 6:71–74
5. Dossi N, Susmel S, Toniolo R, Pizzariello A, Bontempelli G (2009) *Electrophoresis* 30:3465–3471
6. Llopis X, Pumera M, Alegret S, Merkoci A (2009) *Lab Chip* 9:213–218
7. Yi CQ, Zhang Q, Li CW, Yang J, Zhao JL, Yang MS (2006) *Anal Bioanal Chem* 384:1259–1268
8. Viskari PJ, Landers JP (2006) *Electrophoresis* 27:1797–1810
9. Gotz S, Karst U (2007) *Anal Bioanal Chem* 387:183–192
10. Myers FB, Lee LP (2008) *Lab Chip* 8:2015–2031

11. Pennathur S, Fyngenson DK (2008) *Lab Chip* 8:649–652
12. Schwarz MA, Hauser PCS (2001) *Lab Chip* 1:1–6
13. Lu Q, Copper CL, Collins GE (2006) *Anal Chim Acta* 572:205–211
14. Collins GE, Lu Q, Pereira N, Wu P (2007) *Talanta* 72:301–304
15. Salimi-Moosavi H, Jiang Y, Lester L, McKinnon G, Harrison DJ (2000) *Electrophoresis* 21:1291–1299
16. Billot L, Plecis A, Chen Y (2008) *Microelectron Eng* 85:1269–1271
17. Noda T, Takao H, Yoshioka K, Oku N, Ashiki M, Sawada K, Matsumoto K, Ishida M (2006) *Sens Actuators B* 119:245–250
18. Ma B, Zhou X, Wang G, Dai Z, Qin J, Lin B (2007) *Electrophoresis* 28:2474–2477
19. Ou J, Glawdel T, Ren CL, Pawliszyn J (2009) *Lab Chip* 9:1926–1932
20. Petersen NJ, Mogensen KB, Kutter JP (2002) *Electrophoresis* 23:3528–3536
21. Gustafsson O, Mogensen KB, Ohlsson PD, Liu Y, Jacobson SC, Kutter JP (2008) *J Micro-mech Microeng* 18:055021
22. Llobera A, Wilke R, Büttgenbach S (2004) *Lab Chip* 4:24–27
23. Snakenborg D, Mogensen KB, Kutter JP (2003) *Proc Micro Total Anal Syst*:841–844
24. Mogensen KB, Kutter JP (2009) *Electrophoresis* 30:S92–S100
25. Ro KW, Lim K, Shim BC, Hahn JH (2005) *Anal Chem* 77:5160–5166
26. Llobera A, Demming S, Wilke R, Büttgenbach S (2007) *Lab Chip* 7:1560–1566
27. Pan JZ, Yao B, Fang Q (2010) *Anal Chem* 82:3394–3398
28. Prabhakar A, Mukherji S (2010) *Lab Chip* 10:748–754
29. van der Sneppen L, Ariese F, Gooijer C, Ubachs W (2009) *Annu Rev Anal Chem* 2:13–35
30. Waechter H, Litman J, Cheung AH, Barnes JA, Loock H-P (2010) *Sensors* 10:1716–1742
31. Waechter H, Bescherer K, Durr CJ, Oleschuk RD, Loock H-P (2009) *Anal Chem* 81:9048–9054
32. Yao B, Luo G, Wang LD, Gao YD, Lei GT, Ren KN, Chen LX, Wang YM, Hu Y, Qiu Y (2005) *Lab Chip* 5:1041–1047
33. Yao B, Yang HH, Liang QL, Luo G, Wang LD, Ren KN, Gao YD, Wang YM, Qiu Y (2006) *Anal Chem* 78:5845–5850
34. Ren KN, Liang QL, Mu X, Luo GA, Wang YM (2009) *Lab Chip* 9:733–736
35. Fu JL, Fang Q, Zhang T, Jin XH, Fang ZL (2006) *Anal Chem* 78:3827–3834
36. Whiting CE, Dua RA, Duffy CF, Arriaga EA (2008) *Electrophoresis* 29:1431–1440
37. Harrison DJ, Manz A, Fan ZH, Ludi H, Widmer HM (1992) *Anal Chem* 64:1926–1932
38. Harrison DJ, Fluri K, Seiler K, Fan ZH, Effenhauser CS, Manz A (1993) *Science* 261:895–897
39. Ocvirk G, Tang T, Harrison DJ (1998) *Analyst* 123:1429–1434
40. Haab BB, Mathies RA (1999) *Anal Chem* 71:5137–5145
41. Liu SR, Shi YN, Ja WW, Mathies RA (1999) *Anal Chem* 71:566–573
42. Dittrich PS, Manz A (2005) *Anal Bioanal Chem* 382:1771–1782
43. Schiro PG, Kuyper CL, Chiu DT (2007) *Electrophoresis* 28:2430–2438
44. Liang H, Cheng XL, Ma YF (2009) *Anal Chem* 81:2059–2066
45. Sun W, Marchuk K, Wang G, Fang N (2010) *Anal Chem* 82:2441–2447
46. Gai H, Li Y, Silber-Li Z-H, Ma Y, Lin B (2005) *Lab Chip* 5:443–449
47. Le NCH, Yokokawa R, Dao DV, Nguyen TD, Wells JC, Sugiyama S (2009) *Lab Chip* 9:244–250
48. Shi X, Meng X, Sun L, Liu J, Zheng J, Gai H, Yang R, Yeung ES (2010) *Lab Chip* 10:2844–2847
49. Bu X, Chen H, Gai H, Yang R, Yeung ES (2009) *Anal Chem* 81:7507–7509
50. Chen H, Gai H, Yeung ES (2009) *Chem Commun*:1676–1678
51. Yu LF, Huang HQ, Dong XL (2008) *Electrophoresis* 29:5055–5060
52. Klepárník K, Horký M (2003) *Electrophoresis* 24:3778–3783
53. Hellmich W, Pelargus C, Leffhalm K, Ros A, Anselmetti D (2005) *Electrophoresis* 26:3689–3696

54. Hellmich W, Greif D, Pelargus C, Anselmetti D, Ros A (2006) *J Chromatogr A* 1130:195–200
55. Renzi RF, Stamps J, Horn BA, Ferko S, VanderNoot VA, West JAA, Crocker R, Wiedenman B, Yee D, Fruetel JA (2005) *Anal Chem* 77:435–441
56. Novak L, Neuzil P, Pipper J, Zhang Y, Lee SH (2007) *Lab Chip* 7:27–29
57. Kaigala GV, Bercovici M, Behnam M, Elliott D, Santiago JG, Backhouse CJ (2010) *Lab Chip* 10:2242–2250
58. Kim JH, Kim YH, Shin KS, Kim BK, Kim YM, Lee YH, Moon SI, Kim TS, Kang JY, Yang EG, Kim SS, Ju BK, Park JO (2005) A miniaturized fluorescence detection system with an integrated organic light emitting diode. In: *Proceedings 18th IEEE international conference on micro electro mechanical systems*, 30 Jan–3 Feb, Miami, FL, pp 806–809
59. Miyaki K, Guo YL, Shimosaka T, Nakagama T, Nakajima H, Uchiyama K (2005) *Anal Bioanal Chem* 382:810–816
60. Xu J, Xiong Y, Chen SH, Guan YF (2009) *Prog Chem* 21:1325–1334
61. Jang JM, Shin HJ, Hwang SW, Yang EG, Yoon DS, Kim TS, Kang JY (2005) *Sens Actuators B* 108:993–1000
62. Roulet JC, Volkel R, Herzog HP, Verpoorte E, de Rooij NF, Dandliker R (2001) *Opt Eng* 40:814–821
63. Adams M, Enzelberger M, Quake S, Scherer A (2003) *Sens Actuators A* 104:25–31
64. Hashimoto M, Tsukagoshi K, Nakajima R, Kondo K, Arai A (2000) *J Chromatogr A* 867:271–279
65. Su RG, Lin JM, Qu F, Chen ZF, Gao YH, Yamada M (2004) *Anal Chim Acta* 508:11–15
66. Mangru SD, Harrison DJ (1998) *Electrophoresis* 19:2301–2307
67. Lara FJ, Garcia-Campana AM, Velasco AI (2010) *Electrophoresis* 31:1998–2027
68. Hashimoto M, Tsukagoshi K, Nakajima R, Kondo K, Arai A (1999) *Chem Lett*:781–782
69. Garcia-Campana AM, Lara FJ, Gamiz-Gracia L, Huertas-Perez JF (2009) *TrAC Trends Anal Chem* 28:973–986
70. Huang XY, Ren JC (2006) *TrAC Trends Anal Chem* 25:155–166
71. Liu BF, Ozaki M, Utsumi Y, Hattori T, Terabe S (2003) *Anal Chem* 75:36–41
72. Tsukagoshi K, Jinno N, Nakajima R (2005) *Anal Chem* 77:1684–1688
73. Zhao SL, Li XT, Liu YM (2009) *Anal Chem* 81:3873–3878
74. Zhao SL, Huang Y, Liu YM (2009) *J Chromatogr A* 1216:6746–6751
75. Ye FG, Huang Y, Xu Q, Shi M, Zhao SL (2010) *Electrophoresis* 31:1630–1636
76. Zhao SL, Huang Y, Ye FG, Shi M, Liu Y (2010) *J Chromatogr A* 1217:5732–5736
77. Zhao SL, Huang Y, Shi M, Liu RJ, Liu YM (2010) *Anal Chem* 82:2036–2041
78. Wang ZAK, Chin SY, Chin CD, Sarik J, Harper M, Justman J, Sia SK (2010) *Anal Chem* 82:36–40
79. Homola J (2008) *Chem Rev* 108:462–493
80. Furuki M, Kameoka J, Craighead HG, Isaacson MS (2001) *Sens Actuators B* 79:63–69
81. Wheeler AR, Chah S, Whelan RJ, Zare RN (2004) *Sens Actuators B* 98:208–214
82. Liu C, Cui D, Li H (2010) *Biosens Bioelectron* 26:255–261
83. Kurihara K, Ohkawa H, Iwasaki Y, Niwa O, Tobita T, Suzuki K (2004) *Anal Chim Acta* 523:165–170
84. Stöcker P, Menges B, Langbein U, Mittler S (2004) *Sens Actuators A* 116:224–231
85. Levy R, Ruschin S (2007) *Sens Actuators B* 124:459–465
86. Zhang N, Liu H, Knoll W (2009) *Biosens Bioelectron* 24:1783–1787
87. Unfricht DW, Colpitts SL, Fernandez SM, Lynes MA (2005) *Proteomics* 5:4432–4442
88. Huang C, Bonroy K, Reekmans G, Laureyn W, Verhaegen K, De Vlaminck I, Lagae L, Borghs G (2009) *Biomed Microdevices* 11:893–901
89. Cao C, Sim SJ (2009) *Lab Chip* 9:1836–1839
90. Chen LX, Choo J (2008) *Electrophoresis* 29:1815–1828
91. Zhang X, Yin H, Cooper JM, Haswell SJ (2008) *Anal Bioanal Chem* 390:833–840
92. Choi D, Kang T, Cho H, Choi Y, Lee LP (2009) *Lab Chip* 9:239–243
93. Wang M, Jing N, Chou I-H, Coté GL, Kameoka J (2007) *Lab Chip* 7:630–632

94. Chou I-H, Benford M, Beier HT, Coté GL, Wang M, Jing N, Kameoka J, Good TA (2008) *Nano Lett* 8:1729–1735
95. Huh YS, Chung AJ, Cordovez B, Erickson D (2009) *Lab Chip* 9:433–439
96. Cho H, Lee B, Liu GL, Agarwal A, Lee LP (2009) *Lab Chip* 9:3360–3363
97. Tong L, Righini M, González MU, Quidant R, Käll M (2009) *Lab Chip* 9:193–195
98. Quang LX, Lim C, Seong GH, Choo J, Do KJ, Yoo S-K (2008) *Lab Chip* 8:2214–2219
99. Hunt HC, Wilkinson JS (2008) *Microfluid Nanofluid* 4:53–79
100. Hawkins AR, Schmidt H (2008) *Microfluid Nanofluid* 4:17–32
101. Nguyen N-T (2010) *Biomicrofluidics* 4:031501
102. Psaltis D, Quake SR, Yang C (2006) *Nature* 442:381–386
103. Wang SL, Fan XF, Xu ZR, Fang ZL (2005) *Electrophoresis* 26:3602–3608
104. Du WB, Qun F, Fang ZL (2004) *Chem J Univ Chin* 25:610–613
105. Ymeti A, Greve J, Lambeck PV, Wink T, van Hovell S, Beumer TAM, Wijn RR, Heideman RG, Subramaniam V, Kanger JS (2007) *Nano Lett* 7:394–397
106. Crespi A, Gu Y, Nganson B, Hoekstra HJWM, Dongre C, Pollnau M, Ramponi R, van den Vlekkert HH, Watts P, Cerullo G, Osellame R (2010) *Lab Chip* 10:1167–1173
107. Mogensen KB, Kwok YC, Eijkel JCT, Petersen NJ, Manz A, Kutter JP (2003) *Anal Chem* 75:4931–4936
108. Cleary A, Glidle A, Laybourn PJR, García-Blanco S, Pellegrini S, Helfter C, Buller GS, Aitchison JS, Cooper JM (2007) *Appl Phys Lett* 91:071123
109. Sheridan AK, Stewart G, Ur-reyman H, Suyal N, Uttamchandani D (2009) *IEEE Sens J* 9(12):1627–1632
110. Kee JS, Poenar DP, Neuzil P, Yobas L (2008) *Sens Actuators B* 134:532–538
111. Xu F, Datta P, Wang H, Gurung S, Hashimoto M, Wei S, Goettert J, McCarley RL, Soper SA (2007) *Anal Chem* 79:9007–9013
112. Okagbare PI, Emory JM, Datta P, Goettert J, Soper SA (2010) *Lab Chip* 10:66–73
113. Datta A, Eom I-Y, Dhar A, Kuban P, Manor R, Ahmad I, Gangopadhyay S, Dallas T, Holtz M, Temkin H, Dasgupta PK (2003) *IEEE Sens J* 3:788–795
114. Manor R, Datta A, Ahmad I, Holtz M, Gangopadhyay S, Dallas T (2003) *IEEE Sens J* 3:687–692
115. Wu CW, Gong GC (2008) *IEEE Sens J* 8:465–469
116. Cho SH, Godin J, Lo Y-H (2009) *IEEE Photonics Technol Lett* 21:1057–1059
117. Cho SH, Chen CH, Tsai FS, Godin JM, Lo Y-H (2010) *Lab Chip* 10:1567–1573
118. Du WB, Fang Q, He QH, Fang ZL (2005) *Anal Chem* 77:1330–1337
119. Risk W, Kim H, Miller R, Temkin H, Gangopadhyay S (2004) *Opt Express* 12:6446–6455
120. Korampally V, Mukherjee S, Hossain M, Manor R, Yun MS, Gangopadhyay K, Polo-Parada L, Gangopadhyay S (2009) *IEEE Sens J* 9:1711–1718
121. Ligler FS (2009) *Anal Chem* 81:519–526
122. Wolfe DB, Conroy RS, Garstecki P, Mayers BT, Fischbach MA, Paul KE, Prentiss M, Whitesides GM (2004) *Proc Natl Acad Sci USA* 101:12434–12438
123. Rosenauer M, Vellekoop MJ (2009) *Appl Phys Lett* 95:163702
124. Lee KS, Kim SB, Lee KH, Sung HJ, Kim SS (2010) *Appl Phys Lett* 97:021109
125. Mao X, Waldeisen JR, Huang TJ (2007) *Lab Chip* 7:1260–1262
126. Mao X, Lin S-CS, Lapsley MI, Shi J, Juluri BK, Huang T (2009) *Lab Chip* 9:2050–2058
127. Nguyen NT, Kong TF, Goh JH, Low CLN (2007) *J Micromech Microeng* 17:2169–2174
128. Song C, Nguyen N-T, Asundi AK, Tan S-H (2010) *Opt Express* 35:327–329
129. Maselli V, Grenier JR, Ho S, Herman PR (2009) *Opt Express* 17:11719–11729
130. Yin DL, Deamer DW, Schmidt H, Barber JP, Hawkins AR (2006) *Opt Lett* 31:2136–2138
131. Yin DL, Lunt EJ, Rudenko MI, Deamer DW, Hawkins AR, Schmidt H (2007) *Lab Chip* 7:1171–1175
132. Schmidt H, Hawkins AR (2008) *Microfluid Nanofluid* 4:3–16
133. Kuo J-N, Hsieh C-C, Yang S-Y, Lee G-B (2007) *J Micromech Microeng* 17:693–699
134. Camou S, Fujita H, Fujii T (2003) *Lab Chip* 3:40–45

135. Guo HL, Zhao P, Xiao GZ, Zhang ZY, Yao JP (2010) *IEEE J Sel Top Quantum Electron* 16:919–926
136. Hsiung SK, Lee CH, Lee GB (2008) *Electrophoresis* 29:1866–1873
137. Lee JY, Choi ST, Lee SW, Kim WB (2009) *Proc SPIE* 7426:742603
138. Lee SW, Lee SS (2007) *Appl Phys Lett* 90:121129
139. Shi JJ, Stratton Z, Lin SCS, Huang H, Huang TJ (2010) *Microfluid Nanofluid* 9:313–318
140. Mao X, Waldeisen JR, Juluri BK, Huang TJ (2007) *Lab Chip* 7:1303–1308
141. Rosenauer M, Vellekoop MJ (2009) *Lab Chip* 9:1040–1042
142. Tang SKY, Stan CA, Whitesides GM (2008) *Lab Chip* 8:395–401
143. Song C, Nguyen N-T, Tan S-H, Asundi AK (2009) *Lab Chip* 9:1178–1184
144. Song CL, Nguyen NT, Tan SH, Asundi AK (2009) *J Micromech Microeng* 19:085012
145. Huang H, Mao X, Lin SCS, Kiraly B, Huang YP, Huang TJ (2010) *Lab Chip* 10:2387–2393
146. Ohira K, Kobayashi K, Iizuka N, Yoshida H, Ezaki M, Uemura H, Kojima A, Nakamura K, Furuyama H, Shibata H (2010) *Opt Express* 18:15440–15447
147. Vannahme C, Klinkhammer S, Kolew A, Jakobs P-J, Guttmann M, Dehm S, Lemmer U, Mappes T (2010) *Microelectron Eng* 87:693–695
148. Li Z, Psaltis D (2008) *Microfluid Nanofluid* 4:145–158
149. Helbo B, Kristensen A, Menon A (2003) *J Micromech Microeng* 13:307–311
150. Song W, Psaltis D (2010) *Appl Phys Lett* 96:081101
151. Galas JC, Torres J, Belotti M, Kou Q, Chen Y (2005) *Appl Phys Lett* 86:264101
152. Suter JD, Lee W, Howard DJ, Hoppmann E, White IM, Fan XD (2010) *Opt Lett* 35:2997–2999
153. Tang SKY, Li Z, Abate AR, Agresti JJ, Weitz DA, Psaltis D, Whitesides GM (2009) *Lab Chip* 9:2767–2771
154. Balslev S, Kristensen A (2005) *Opt Express* 13:344–351
155. Li ZY, Zhang ZY, Emery T, Scherer A, Psaltis D (2006) *Opt Express* 14:696–701
156. Gersborg-Hansen M, Kristensen A (2006) *Appl Phys Lett* 89:103518
157. Song W, Vasdekis AE, Li Z, Psaltis D (2009) *Appl Phys Lett* 94:051117
158. Vannahme C, Christiansen MB, Mappes T, Kristensen A (2010) *Opt Express* 18:9280–9285
159. Chabinye ML, Chiu DT, McDonald JC, Stroock AD, Christian JF, Karger AM, Whitesides GM (2001) *Anal Chem* 73:4491–4498
160. Webster JR, Burns MA, Burke DT, Mastrangelo CH (2001) *Anal Chem* 73:1622–1626
161. Kamei T, Paegel BM, Scherer JR, Skelley AM, Street RA, Mathies RA (2003) *Anal Chem* 75:5300–5305
162. Pereira AT, Pimentel AC, Chu V, Prazeres DMF, Conde JP (2009) *IEEE Sens J* 9:1282–1290
163. Hofmann O, Miller P, Sullivan P, Jones TS, de Mello JC, Bradley DDC, de Mello AJ (2005) *Sens Actuators B* 106:878–884
164. Wang X, Hofmann O, Das R, Barrett EM, Demello AJ, Demello JC, Bradley DDC (2007) *Lab Chip* 7:58–63
165. Wang X, Amaratongchai M, Nacapricha D, Hofmann O, de Mello JC, Bradley DDC, de Mello AJ (2009) *Sens Actuators B* 140:643–648
166. Pais A, Banerjee A, Klotzkin D, Papautsky I (2008) *Lab Chip* 8:794–800
167. Wojciechowski JR, Shriver-Lake LC, Yamaguchi MY, Fureder E, Pieler R, Schamesberger M, Winder C, Prall HJ, Sonnleitner M, Ligler FS (2009) *Anal Chem* 81:3455–3461
168. Lange D, Storment CW, Conley CA, Kovacs GTA (2005) *Sens Actuators B* 107:904–914
169. Heng X, Erickson D, Baugh LR, Yaqoob Z, Sternberg PW, Psaltis D, Yang C (2006) *Lab Chip* 6:1274–1276
170. Cui XQ, Lee LM, Heng X, Zhong WW, Sternberg PW, Psaltis D, Yang CH (2008) *Proc Natl Acad Sci USA* 105:10670–10675
171. Pang S, Cui X, DeModena J, Wang YM, Sternberg PW, Yang CH (2010) *Lab Chip* 10:411–414
172. Vig AL, Marie R, Jensen E, Kristensen A (2010) *Opt Express* 18:4158–4169
173. Zheng G, Lee SA, Yang S, Yang C (2010) *Lab Chip* 10:3125–3129